CARBON letters

Original Articles
Carbon Letters Vol. 24, 97-102 (2017)

Graphitization of PAN-based carbon fibers by CO_2 laser irradiation

Liangbo Yao[1], Weimin Yang[1], Sanyang Li[1], Yang Sha[2], Jing Tan[1,♣], Ying An[1] and Haoyi Li[1]

[1]College of Mechanical and Electrical Engineering, Beijing University of Chemical Technology, Beijing 100029, China
[2]National Carbon Fiber Engineering Research Center, Beijing University of Chemical Technology, Beijing 100029, China

Article Info

Received 18 May 2017
Accepted 17 August 2017

♣Corresponding Author
E-mail: tanj@mail.buct.edu.cn
Tel: +86-10-64434734

Open Access

DOI: http://dx.doi.org/10.5714/CL.2017.24.097

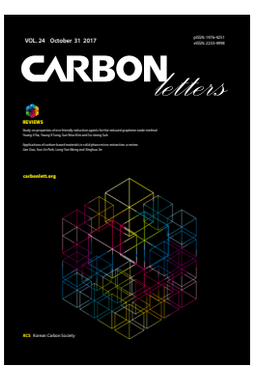

http://carbonlett.org

pISSN: 1976-4251
eISSN: 2233-4998

Abstract

Graphite fibers are materials with a high specific modulus that have attracted much interest in the aerospace industry, but their high manufacturing cost and low yield are still problems that prevent their wide applications in practice. This paper presents a laser-based process for graphitization of carbon fiber (CF) and explores the effect of laser radiation on the microstructure of CF. The obtained Raman spectra indicate that the outer surface of CF evolves from turbostratic structures into a three-dimensional ordered state after being irradiated by a laser. The X-ray diffraction data revealed that the growth of crystallite was parallel to the fiber axis, and the interlayer spacing d_{002} decreased from 0.353 to 0.345 nm. The results of scanning electron microscopy revealed that the surface of irradiated CFs was rougher than that of the unirradiated ones and there were scale-like small fragments that had peeled off from the fibers. The tensile modulus increased by 17.51% and the Weibull average tensile strength decreased by 30.53% after being irradiated by a laser. These results demonstrate that the laser irradiation was able to increase the graphitization degree of the CFs, which showed some properties comparable to graphite fibers.

Key words: carbon fiber, graphitization, microstructure, laser irradiation

1. Introduction

Graphite fibers have a wide range of applications in aerospace, military and high-tech industries due to their excellent mechanical, electronical and thermal properties [1,2]. The graphitization of carbon fibers (CFs) is traditionally done in special and costly devices, such as high temperature electric resistance furnaces, arc furnaces and induction furnaces. Great efforts have been made to reduce the costs and energy assumption by introducing various kinds of high energy heat sources to irradiate CFs. Xu et al. [3] improved the graphitization degree of polyacrylonitrile (PAN)-based carbon fibers by gamma ray irradiation at a 2 mGy dose. Wang et al. [4] invented a microwave-based manufacturing method which is capable of producing PAN-based graphite fibers with higher crystalline stacking size Lc and lower crystalline planar size La compared to conventional CFs.

Lasers are also a kind of heat source which may be a candidate for the graphitization of CFs. Lott et al. [5] used a laser for the stabilization and carbonization of the carbonaceous precursor fibers and found that the laser-based process had a higher accessible heating rates without thermal damage to the fibers than the conventional furnace based approach. Go et al. [6] found that the infrared laser-induced carbonization of PAN-nanofiber mats was able to get much higher surface areas and smaller pores than the classical thermal carbonization methods. Blaker et al. [7] modified the structure of CFs using a laser, obtaining increased pullout characteristics, better fiber surface and an expanded graphitization region at the predetermined points. All these previous studies indicate that it is possible to enhance the graphitization of CFs by laser irradiation.

In this study, PAN-based carbon fibers were graphitized with a CO_2 laser to determine the

feasibility of laser-based graphitization of CFs. We studied the surface microstructure, surface morphology and mono-filament mechanical properties of CFs after laser irradiation. Raman spectroscopy, X-ray diffraction (XRD) and a scanning electron microscope (SEM) were used to characterize the surface structure and morphology after laser irradiation.

2. Experimental

The CFs (1 k) used for graphitizing, which had been heat-treated to approximately 1300°C without sizing treatment on the surface, were about 1 mm in diameter. The schematic of the device used in the experiments is shown in Fig. 1. Continuous CO_2 laser irradiation with a wavelength of 10.6 μm and a maximum output power of 180 W was applied in all experiments. The laser beam was about 2 mm in diameter. The temperature of the laser spot on the CFs was able to be controlled by monitoring the output power of the laser. In the graphitization process, a bundle of CF was passed through a special apparatus at a constant rate (0.4 mm s^{-1}) and heated up to about 2100°C in a short time by laser irradiation at a power of 63 W under the protection of an argon atmosphere (O_2 <0.2 ppm and 3 ppm at the inlet and exit, respectively). The temperature of laser spot on the CF was measured by a IR thermometer (Marathon MM series; Raytek, Japan). The argon was provided by an RZ-YA-4D argon gas purifier manufactured by the Suzhou RuiZe gas purification equipment Co., Ltd, China. The oxygen content at the exit was measured by a CW2000ZX fuel-cell trace oxygen analyzer produced by Beijing Oxygenwind Technology Exploiture Center (China). To keep the fiber in a stretched state during the heat treatment, a draw weight of 50 g was applied.

The Raman spectra of the CFs were measured by a RM2000 micro-confocal Raman spectrometer (Renishaw, UK) and a 532 nm line from an argon laser was used as an excitation source. All spectra were recorded at room temperature. Additionally, the crystal structures of CFs were characterized by XRD (PANalytical B.V, the Netherlands, Cu Kα, λ=1.54178 Å). The morphology images of the samples were taken by SEM (Hitachi-S-7800, Japan). All the results were averaged over five independent samples.

The mechanical properties were measured for twenty individual fibers with a gauge length of 25 mm [8]. The diameter of individual fibers was measured by optical microscopy. The fiber samples were randomly selected from the fiber bundle and were fixed by an instant adhesive (colophony) on the paper holders. The samples together with the paper holder were mounted on a tensile apparatus (YG001A; Taicang textile equipment factory, China) and the paper frame was cut off before the samples were stretched. The samples were extended to break at the rate of 2 mm/min. The tensile modulus and elongation at break were averaged over all the measured samples.

3. Results and Discussion

3.1. Raman analysis

Fig. 2a and b present the Raman spectra for the CFs with and without laser treatment, respectively. Deconvolution with a Lorentzian curve [9-11] was used to analyze the spectra of as-received carbon fiber for detailed structural formation, and the results are shown in Fig. 2a. The deconvolution peaks reveal that the surface structure of the CF is graphite-like in the area of the laser spot, where a disordered sp^2 lattice (peak D2, 1612 cm^{-1}), amorphous carbon structures (peak D3, 1489 cm^{-1}) and polyene-like structures (peak D4, 1193 cm^{-1}) coexist in pristine CFs [12,13]. Fig. 2b shows that the peak values of full width at half maximum (FWHM) for the D and G bands decrease distinctly, which suggest that the structure defects and disordered carbonaceous components of the CFs decreased and the graphite-like structures evolved into three-dimensional ordered states after being irradiated by lasers. Meanwhile, the ID/IG intensity ratio decreased from 1.4515 to 0.0811, which also suggests an increase of ordered graphite crystallites. These results are consistent with that of a previous study [14].

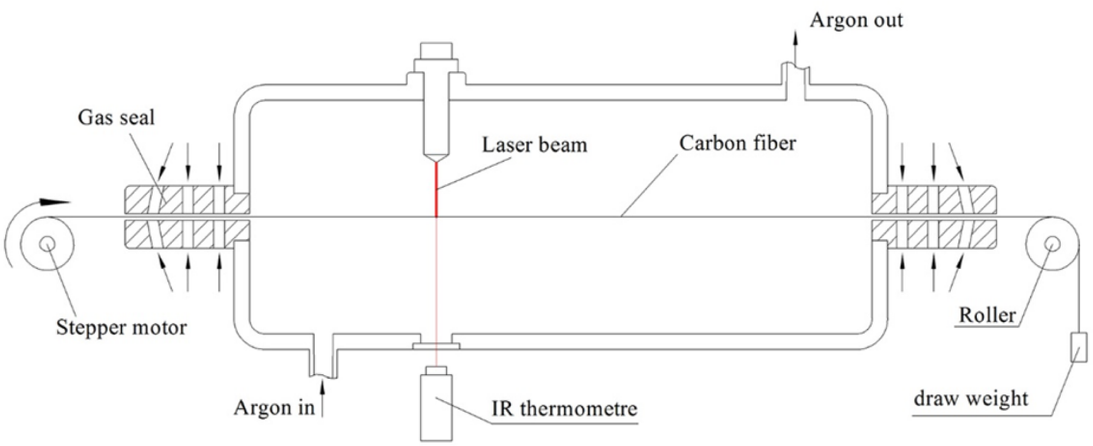

Fig. 1. The laser irradiation experimental setup used in the graphitization process.

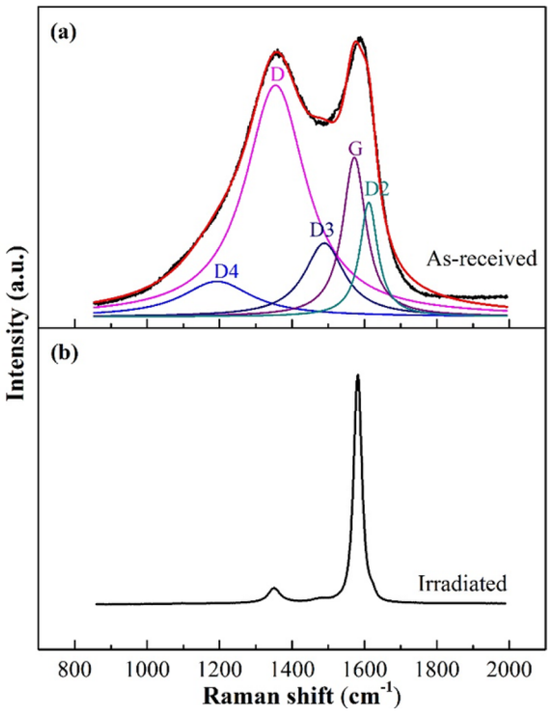

Fig. 2. Raman spectrum of as-received (a) and laser irradiated (b) carbon fibers.

3.2. XRD analysis

The XRD patterns of the two series of CFs were normalized by their integration in the range of scanning angle and are shown in Fig. 3. The equatorial scan patterns in Fig. 3a have peaks around 26°, 43°, and 53°, which correspond to the (002), (10), (004) of carbon structures, respectively. After being irradiated by a laser, the (002) peak moved towards a higher 2θ angle, which means the interlayer spacing decreased. The peak also becomes narrower and sharper, showing an increased intensity, which suggests that larger crystallites were formed after the laser irradiation. This observation is in good agreement with the Raman spectra in Fig. 2 in which the G band is intensified by the laser irradiation. The partial and enlarged equatorial scan patterns in the 2θ ranges of 38–56° and 74–90° are shown in Fig. 3b. The splitting of peak (10) and appearance of peak (112) in the equatorial scan after irradiation can be attributed to the appearance of three-dimensional graphitic crystallinity in the CFs [15]. Meanwhile, the narrower and sharper peak (004) indicates that the graphite micro-crystals tend to grow along the direction of the carbon axis [16].

The corresponding results are listed in Table 1 according to the XRD patterns. Compared with the untreated fibers, the spacing of graphite layers of irradiated fibers (0.345 nm) was closer to the ideal value for a perfect graphite crystal (0.335 nm), which indicates that the average graphitization of the treated fibers was improved by laser irradiation. The graphene-layer stacking height Lc, the transverse crystallite width $La_{\perp}$, the number of lattices and the degree of orientation (π) increased, which means

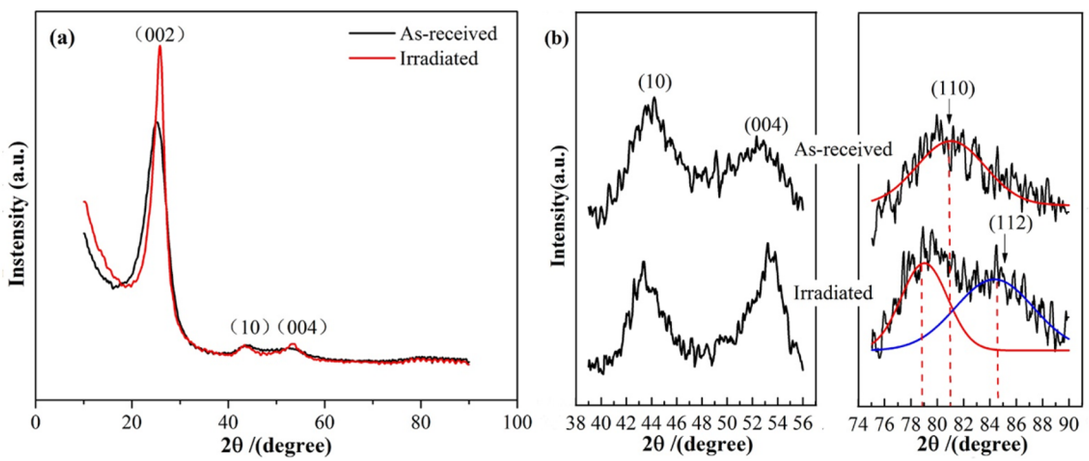

Fig. 3. XRD patterns of as-received and laser irradiated carbon fibers: (a) equatorial and (b) enlarged equatorial scan in the (10) and (110) regions. XRD, X-ray diffraction.

Table 1. Crystallite parameters of pristine and laser irradiated PAN-based carbon fibers

Type	Peak 002		L_C (nm)	Peak 10		No. of lattices	π (%)
	2θ (°)	d_{002} (nm)		2θ (°)	L_a (nm)		
As-received	25.654	0.353	1.709	43.063	5.015	5	81.9
Irradiated	25.817	0.345	2.971	42.931	8.411	9	86.1

PAN, polyacrylonitrile.

that microcrystalline structures evolved into graphite structures, which agrees well with the Raman results.

3.3. Surface morphology analysis

The surface morphologies of pristine and irradiated PAN-based CFs are shown in Fig. 4a and b, respectively. The surface of the irradiated CFs was rougher than that of the pristine CFs, which was likely due to the laser etching process on the CF surface. As shown in Fig. 4b, there were scale-like small fragments peeled off from the original fibers, as well as some cracks that formed preferentially along the fiber axis. This perceptible exfoliation may be have been caused by the rapid temperature increase of the carbon fiber under laser irradiation and the sharp spillage of non-carbon elements [7,17], or by the cleaving between the hexagonal carbon layers, like the exfoliation of natural graphite flakes [17]. Similarly, a previous study indicated that pre-exfoliation promotes the graphitization of CFs during high temperature treatment [18]. However, the exact causes and mechanisms for the exfoliation in this study are still in need of further investigations.

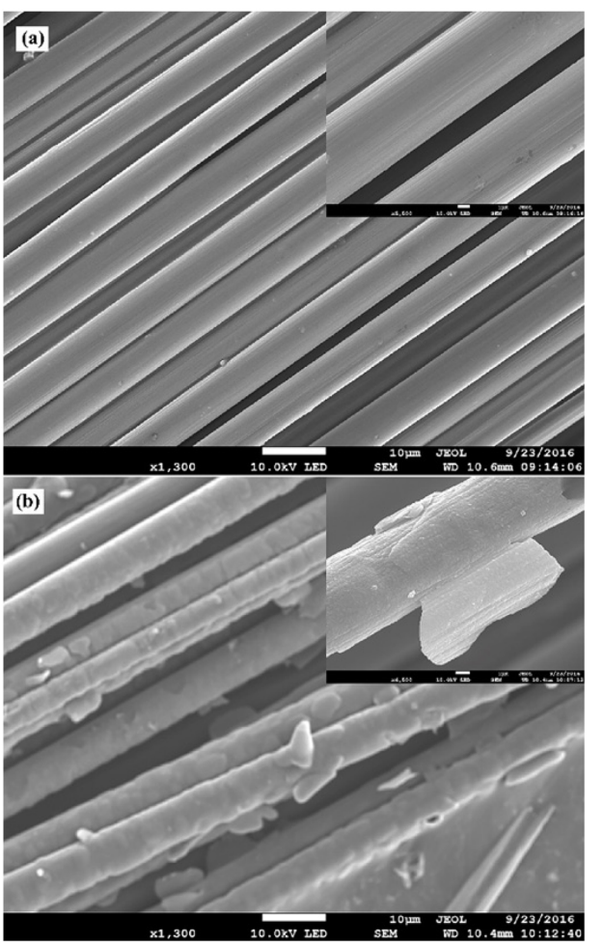

Fig. 4. SEM micrographs of as-received (a) and laser irradiated (b) PAN-based carbon fibers. SEM, scanning electron microscope; PAN, polyacrylonitrile.

3.4. Mechanical properties

The results for the two series of mechanical tests were analyzed based on a single modal two-parameter Weibull distribution function (applicable to brittle material) as shown in Eq. 1 [19,20]. Fig. 5 shows the cumulative frequency of the tensile strength (black discrete point) and Weibull plot (red line), which is expressed as

$$F(\sigma) = 1 - exp\left[-(\frac{\sigma}{\sigma_0})^m\right] \quad (1)$$

, where $F(\sigma)$ is the probability of failure up to the stress level σ, σ_0 is the Weibull scale parameter. The Weibull modulus (Weibull shape parameter) m indicates the degree of scatter on the strength. In addition, the mean ($\bar{\sigma}$), standard deviation (S) and coefficient of variation (C_v) can be derived from Eq. 1,

$$\bar{\sigma} = \sigma_0 \Gamma\left(1 + \frac{1}{m}\right) \quad (2)$$

$$S = \sigma_0 \sqrt{\Gamma\left(1 + \frac{2}{m}\right) - \Gamma^2\left(1 + \frac{1}{m}\right)} \quad (3)$$

$$C_v = \frac{S}{\bar{\sigma}} = \frac{\sqrt{\Gamma\left(1+\frac{2}{m}\right) - \Gamma^2\left(1+\frac{1}{m}\right)}}{\Gamma\left(1+\frac{1}{m}\right)} \quad (4)$$

, where Γ represents the Gamma function

$$\Gamma(S) = \int_0^{+\infty} e^{-x} x^{S-1} dx \ (S > 0) \quad (5)$$

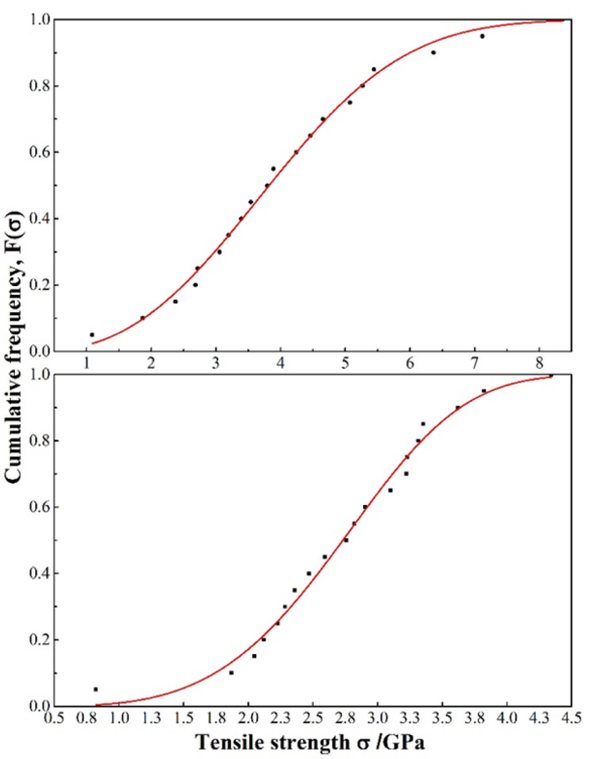

Fig. 5. Numerical fitting curves of the single fiber tensile strength of carbon fibers before (a) and after (b) irradiation.

Table 2. Weibull parameters and tensile properties of the single fiber tensile strength of carbon fibers

Fiber type	Average diameter d (μm)	Weibull modulus m	Scale parameter σ_0 (GPa)	Weibull average tensile strength $\bar{\sigma}$ (GPa)	Average tensile strength σ (GPa)	Tensile modulus E (GPa)	Elongation at break (%)	S	C_v (%)
As-received	6.805	2.665	4.385	3.898	4.129	221.482	1.852	1.575	40.41
Irradiated	6.043	4.184	2.98	2.708	2.765	260.265	1.088	0.729	26.94

The fitted results and related parameters for all the investigated fibers are summarized in Table 2. The tensile strength, tensile modulus and elongation at break were averaged over all the measured samples. The results clearly show that CFs after laser irradiation had a higher Weibull modulus and the tensile modulus was increased by 17.51%, while the average diameter, the Weibull average tensile strength and elongation at break were reduced by 11.2, 30.53, and 41.25%, respectively. For the PAN-based carbon fibers, the presence of surface defects (including the distorted shape of the fiber) affected their tensile strength and Weibull modulus [8]. Higher values of the Weibull modulus indicated that there were more surface defects and these defects were distributed more uniformly throughout the material after laser irradiation, which resulted in a smaller scatter in the tensile strength. These results are consistent with the SEM images shown in Fig. 4.

4. Conclusions

In this study, a laser-based graphitizing process was proposed, and the microstructure, morphology and mechanical properties of the laser-irradiated CFs were characterized by Raman spectroscopy, XRD, SEM, and tensile experiments. The results indicated that the chemical and crystallite structures evolved into graphite structures after the CFs were irradiated by a laser. Additionally, the fiber diameter showed 11.5% shrinkage, which resulted in a rougher fiber surface and scale-like small fragments peeled off from the fibers. The single modal two-parameter Weibull distributions of tensile strengths for the measured fibers show an increase in Weibull modulus and a decrease in scale parameters, indicating a higher probability of surface defects. The tensile modulus increased by 17.51%, while the tensile strength decreased to about 2.765 GPa. These data demonstrate that the fibers after laser treatment had properties comparable to graphite fiber. Further studies on the influence of the processing parameters like laser wavelength, hold time, heating rates, and draw weights on the mechanical properties of the CFs need to be carried out to achieve further improvement.

Conflict of Interest

No potential conflict of interest relevant to this article was reported.

Acknowledgments

This work was financially supported by the National Natural Science Foundation of China under Grant No. 51602015. The authors would like to thank associate Prof. Weiyu Cao of the National Carbon Fiber Engineering Research Center at Beijing University of Chemical Technology for providing the carbonized PAN-carbon fibers and Dr. Lisheng Cheng for his research guidance.

References

[1] Kim KW, Lee HM, Kim BS, Hwang SH, Kwac LK, An KH, Kim BS. Preparation and thermal properties of polyethylene-based carbonized fibers. Carbon Lett, **16**, 62 (2015). https://doi.org/10.5714/CL.2015.16.1.062.

[2] Baral N, Guezenoc H, Davies P, Baley C. High modulus carbon fibre composites: correlation between transverse tensile and mode I interlaminar fracture properties. Mater Lett, **62**, 1096 (2008). https://doi.org/10.1016/j.matlet.2007.07.071.

[3] Xu Z, Liu L, Huang Y, Sun Y, Wu X, Li J. Graphitization of polyacrylonitrile carbon fibers and graphite irradiated by γ rays. Mater Lett, **63**, 1814 (2009). https://doi.org/10.1016/j.matlet.2009.05.055.

[4] Wang CY, Liu IW, Chen JP, Cheng SH, Cheng SY. High modulus graphitized carbon fiber and method for fabricating the same. US Patent 8,906,339 (2014).

[5] Lott P, Stollenwerk J, Wissenbach K. Laser-based production of carbon fibers. J Laser Appl, **27**, S29106 (2015). https://doi.org/10.2351/1.4906476.

[6] Go D, Lott P, Stollenwerk J, Thomas H, Möller M, Kuehne AJC. Laser carbonization of PAN-nanofiber mats with enhanced surface area and porosity. ACS Appl Mater Interfaces, **8**, 28412 (2016). https://doi.org/10.1021/acsami.6b09358.

[7] Blaker JJ, Anthony DB, Tang G, Shamsuddin SR, Kalinka G, Weinrich M, Abdolvand A, Shaffer MSP, Bismarck A. Property and shape modulation of carbon fibers using lasers. ACS Appl Mater Interfaces, **8**, 16351 (2016). https://doi.org/10.1021/acsami.6b05228.

[8] Naito K, Tanaka Y, Yang JM, Kagawa Y. Tensile properties of ultrahigh strength PAN-based, ultrahigh modulus pitch-based and high ductility pitch-based carbon fibers. Carbon, **46**, 189 (2008). https://doi.org/10.1016/j.carbon.2007.11.001.

[9] Yoo SH, Jang D, Joh HI, Lee S. Iron oxide/porous carbon as a heterogeneous Fenton catalyst for fast decomposition of hydrogen peroxide and efficient removal of methylene blue. J Mater Chem A, **5**, 748 (2017). https://doi.org/10.1039/C6TA07457J.

[10] Li N, Wu Z, Huo L, Zong L, Guo Y, Wang J, Jian X. One-step functionalization of carbon fiber using in situ generated aromatic diazonium salts to enhance adhesion with PPBES resins. RSC Adv, **6**, 70704 (2016). https://doi.org/10.1039/C6RA12717G.

[11] Sadezky A, Muckenhuber H, Grothe H, Niessner R, Pöschl U. Raman microspectroscopy of soot and related carbonaceous materials: spectral analysis and structural information. Carbon, **43**, 1731 (2005). https://doi.org/10.1016/j.carbon.2005.02.018.

[12] Wang Y, Alsmeyer DC, McCreery RL. Raman spectroscopy of carbon materials: structural basis of observed spectra. Chem Mater, **2**, 557 (1990). https://doi.org/10.1021/cm00011a018.

[13] Marshall CP, Edwards HGM, Jehlicka JJ. Understanding the application of Raman spectroscopy to the detection of traces of life. Astrobiology, **10**, 229 (2010). https://doi.org/10.1089/ast.2009.0344.

[14] Pimenta MA, Dresselhaus G, Dresselhaus MS, Cançado LG, Jorio A, Saito R. Studying disorder in graphite-based systems by Raman spectroscopy. Phys Chem Chem Phys, **9**, 1276 (2007). https://doi.org/10.1039/B613962K.

[15] Ogale AA, Lin C, Anderson DP, Kearns KM. Orientation and dimensional changes in mesophase pitch-based carbon fibers. Carbon, **40**, 1309 (2002). https://doi.org/10.1016/S0008-6223(01)00300-1.

[16] Dobiášová L, Starý V, Glogar P, Valvoda V. Analysis of carbon fibers and carbon composites by asymmetric X-ray diffraction technique. Carbon, **37**, 421 (1999). https://doi.org/10.1016/S0008-6223(98)00207-3.

[17] Voisey KT, Fouquet S, Roy D, Clyne TW. Fibre swelling during laser drilling of carbon fibre composites. Opt Lasers Eng, **44**, 1185 (2006). https://doi.org/10.1016/j.optlaseng.2005.10.008.

[18] Toyoda M, Shimizu A, Iwata H, Inagaki M. Exfoliation of carbon fibers through intercalation compounds synthesized electrochemically. Carbon, **39**, 1697 (2001). https://doi.org/10.1016/S0008-6223(00)00293-1.

[19] Weibull W. Wide applicability. J Appl Mech, **18**, 293 (1951).

[20] Naito K, Oguma H. Tensile properties of novel carbon/glass hybrid thermoplastic composite rods. Compos Struct, **161**, 23 (2017). https://doi.org/10.1016/j.compstruct.2016.11.042.